0026-895X/10/7802-205–214$20.00
MOLECULAR PHARMACOLOGY
Vol. 78, No. 2
64253/3607739
Mol Pharmacol 78:205–214, 2010
Printed in U.S.A.

Prediction of Functionally Selective Allosteric Interactions at an M_3 Muscarinic Acetylcholine Receptor Mutant Using *Saccharomyces cerevisiae*

Gregory D. Stewart, Patrick M. Sexton, and Arthur Christopoulos

Drug Discovery Biology, Monash Institute of Pharmaceutical Sciences & Department of Pharmacology, Monash University, Parkville, Victoria, Australia

Received February 17, 2010; accepted May 12, 2010

ABSTRACT

Saccharomyces cerevisiae is a tractable yeast species for expression and coupling of heterologous G protein-coupled receptors with the endogenous pheromone response pathway. Although this platform has been used for ligand screening, no studies have probed its ability to predict novel pharmacology and functional selectivity of allosteric ligands. As a proof of concept, we expressed a rat M_3 muscarinic acetylcholine receptor (mAChR) bearing a mutation ($K^{7.32}E$) recently identified to confer positive cooperativity between acetylcholine and the allosteric modulator brucine in various strains of *S. cerevisiae*, each expressing a different human Gα/yeast Gpa1 protein chimera, and probed for G protein-biased allosteric modulation. Subsequent assays performed in this system revealed that brucine was a partial allosteric agonist and positive modulator of carbachol when coupled to Gpa1/G_q proteins, a positive modulator (no agonism) when coupled to Gpa1/G_{12} proteins, and a neutral modulator when coupled to Gpa1/G_i proteins. It is noteworthy that these results were validated at the human $M_3K^{7.32}E$ mAChR expressed in a mammalian (Chinese hamster ovary) cell background by determination of calcium mobilization and membrane ruffling as surrogate measures of G_q and G_{12} protein activation, respectively. Furthermore, the combination of this functionally selective allosteric modulator with G protein-biased yeast screens allowed us to ascribe a potential G protein candidate (G_{12}) as a key mediator for allosteric modulation of $M_3K^{7.32}E$ mAChR-mediated ERK1/2 phosphorylation, which was confirmed by small interfering RNA knockdown experiments. These results highlight how the yeast platform can be used to identify functional selectivity of allosteric ligands and to facilitate dissection of convergent signaling pathways.

The five subtypes (M_1–M_5) of muscarinic acetylcholine receptors (mAChRs) are prototypical members of family A G protein-coupled receptors (GPCRs) (Caulfield, 1993). The M_1, M_4, and M_5 mAChRs are predominantly expressed in the CNS, whereas M_2 and M_3 mAChRs are expressed widely in the CNS and periphery (Wess et al., 2007). Of these receptors, the M_3 mAChR currently represents the predominant subtype with respect to established clinical therapies, having proven a tractable drug target for conditions such as chronic obstructive pulmonary disease and overactive bladder disorder (Wess et al., 2007). Nonetheless, subtype-selective targeting of mAChRs remains difficult because of the high degree of sequence conservation in the orthosteric binding site (Caulfield, 1993; Gregory et al., 2007). One approach to circumvent this issue is to target alternative allosteric sites on these receptors (Birdsall and Lazareno, 2005).

Although mAChRs are known to possess more than one allosteric site (Christopoulos et al., 1998; Gregory et al., 2007), most studies thus far have focused on the so-called "prototypical" allosteric site, which binds neuromuscular blocking agents (such as gallamine and alcuronium), alkane-bis-ammonium compounds (including heptane-1,7-bis-dimethyl-3′-phthalimidopropyl ammonium bromide), and alkaloid derivatives (such as brucine). This prototypical mAChR allosteric site is thought to encompass regions of the receptor's second and third extracellular loops and the top of transmembrane (TM) domain VII (Gnagey et al., 1999; Avlani et al., 2007; Gregory et al., 2007; May et al., 2007). In particular, amino acid residue 523 [7.32; Ballesteros and Weinstein (1992) nomenclature], at the junction of TMVII and the third extracellular loop of the human

This work was funded by the National Health and Medical Research Council (NHMRC) of Australia [Program Grant 519461]. Arthur Christopoulos is a Senior, and Patrick Sexton a Principal, Research Fellow of the NHMRC. Gregory Stewart is the recipient of an Australian Postgraduate Award (Industry) from the Australian Research Council.

Article, publication date, and citation information can be found at http://molpharm.aspetjournals.org.

doi:10.1124/mol.110.064253.

ABBREVIATIONS: mAChR, muscarinic acetylcholine receptor; GPCR, G protein-coupled receptor; TM, transmembrane; CCh, carbachol; NMS, *N*-methyl scopolamine; CHO, Chinese hamster ovary; AM, acetoxymethyl; DMEM, Dulbecco's modified Eagle's medium; FBS, fetal bovine serum; siRNA, small interfering RNA; ERK, extracellular signal-regulated kinase; PTX, pertussis toxin; r, rat; ANOVA, analysis of variance.

mAChR, plays an important role in the binding and cooperativity of prototypical allosteric ligands (Gnagey et al., 1999; Krejcí and Tucek, 2001; Jakubík et al., 2005). It is noteworthy that a recent study by Iarriccio (2008) found that substitution of $Lys^{7.32}$ on the M_3 mAChR with $Glu^{7.32}$, the M_1 mAChR equivalent, resulted in positive cooperativity between the allosteric modulator brucine and the endogenous agonist acetylcholine compared with the wild-type M_3 mAChR, where brucine displays almost neutral cooperativity with the agonist.

The ability of a single amino acid substitution to profoundly change the nature of an allosteric interaction between a small-molecule modulator and the endogenous orthosteric agonist is consistent with the highly dynamic nature of GPCRs, which exhibit substantial pleiotropy with respect to both extracellular ligands and intracellular effector pathways. An important paradigm associated with this conformational plasticity of GPCRs is the phenomenon dubbed "functional selectivity," whereby different ligands can promote unique conformations that bias the receptor stimulus toward certain pathways but exclude others (Kenakin, 1995; Urban et al., 2007). Because allosteric ligands, by their very nature, alter the conformation of the receptor in the absence and presence of an orthosteric ligand, it may be expected that such molecules will have the propensity to engender functional selectivity in the actions of orthosteric ligands (Leach et al., 2007). However, the detection of functionally selective ligands, be they orthosteric or allosteric, poses a substantial challenge to modern drug discovery because of the general necessity to probe different signaling pathways in different cell backgrounds.

We have explored the utility of the yeast system *Saccharomyces cerevisiae* as a sensor of GPCR-G protein coupling preferences that may be predictive of signaling patterns operative in mammalian cellular backgrounds (Stewart et al., 2009, 2010). The utility of using this system to study mammalian GPCR/G protein interactions was first demonstrated in studies of β_2-adrenergic receptor coupling to mammalian $G\alpha_s$ proteins (King et al., 1990). Since then, further modifications to the yeast system have been made to accommodate mammalian GPCR signaling. One pivotal modification is the expression of a chimera consisting of Gpa1 (yeast $G\alpha$ protein) with a five C-terminal amino acid substitution from the mammalian $G\alpha$ protein of choice (Brown et al., 2000; Dowell and Brown, 2002). Using this approach, we uncovered novel G protein-biased signaling of M_3 mAChR ligands (such as atropine) previously classed as traditional orthosteric "antagonists" that was subsequently validated in mammalian cells (Stewart et al., 2010). This exciting finding prompted the current study, in which we investigated whether the *S. cerevisiae* platform could also be used to identify allosteric ligand-mediated functional selectivity, at the level of the G protein. As a proof of concept, we focused on the brucine-carbachol (CCh) interaction at the $K^{7.32}E$ M_3 mAChR mutant. We reveal that the yeast system is 1) indeed capable of identifying G protein pathway-selective allosteric modulation that is predictive of behavior in mammalian cells and 2) is also a potentially useful tool to help unravel networks of convergent signaling in mammalian cells.

Materials and Methods

Materials. The *Surefire* ERK1/2 phosphorylation kit was kindly donated by Dr. Michael Crouch (TGR BioSciences, Thebarton, SA, Australia). The p416GPD $rM_3\Delta i3$ mAChR was a generous gift from Dr. Jürgen Wess (National Institute of Diabetes and Digestive and Kidney Diseases, Bethesda, MD). The yeast strains were a kind gift from Dr. Simon Dowell (GlaxoSmithKline, Stevenage, UK). AlphaScreen beads and ^{3}H-labeled *N*-methyl scopolamine ([^{3}H]NMS), were purchased from PerkinElmer Life and Analytical Sciences (Waltham, MA). Flp-In Chinese hamster ovary (CHO) cells, Gateway plasmids, BP clonase kit, LR clonase kit, hygromycin B, Zeocin, Fluo-4-AM, *S. cerevisiae* EasyComp transformation kit, Lipofectamine 2000 reagent, fluorescein di(β-D-galactopyranoside), Fluo-4-AM, Hoechst 33342, Alexa Fluor 568-conjugated phalloidin, and Dulbecco's modified Eagle's medium (DMEM) were obtained from Invitrogen (Carlsbad, CA). cDNA constructs of the human M_3 mAChR were purchased from the Missouri University of Science and Technology (Missouri S&T; http://cdna.org). Fetal bovine serum (FBS) was purchased from JRH Biosciences (Lenexa, KS). $G\alpha_q$ or $G\alpha_{12}$ siRNAs were acquired from Ambion (Austin, TX). All other reagents were purchased from Sigma Aldrich (St. Louis, MO).

Yeast Transformations and Signaling Assay. *S. cerevisiae* strains expressing chimeras of five C-terminal amino acids of human $G\alpha$ protein with Gpa1 (1–467) have been described previously (Brown et al., 2000). The yeast strains were further transformed with a p416GPD vector containing the gene encoding the rat M_3 muscarinic acetylcholine receptor ($rM_3\Delta i3$ mAChR) with an intracellular 3rd loop deletion described by Erlenbach et al. (2001), using the *S. cerevisiae* EasyComp transformation kit in accordance with manufacturer's instructions (Invirogen). The $K^{7.32}E$ ($K^{522}E$) mutation was introduced by site-directed mutagenesis using the QuikChange mutagenesis kit (Stratagene, La Jolla, CA) by annealing the following oligodeoxynucleotide pair into the open vector: 5′-GACAGCTGCATACCCGAAACCTATTGGAATC 3′ and 5′-GATTCCAATAGGTTTCGGGTATGCAGCTGTC-3′. The vector containing the mutated gene was then transformed in the manner described above.

The conditions for the signaling component of the assay have also been described previously (Olesnicky et al., 1999). In brief, single colonies were cultured overnight at 30°C in synthetic complete (SC) medium, lacking amino acids required for plasmid maintenance. Cells were pelleted and diluted to 0.02 OD_{600} mL^{-1} in synthetic complete medium, lacking amino acids, but supplemented with 0 to 10 mM 3-aminotriazole, 1 μM fluorescein di(β-D-galactopyranoside), and 0.1 M sodium phosphate, pH 7.3. Cell suspensions were diluted into 96-well plates with various ligands and incubated for 18 to 24 h at 30°C. Fluorescence was measured in a Flexstation (Molecular Devices Sunnyvale, CA) using an excitation wavelength of 485 nm and an emission wavelength of 520 nm.

Transfections and Cell Culture. The cDNA sequence of the human M_3 mAChR was amplified by polymerase chain reaction and cloned, using classic cloning methods, into the Gateway entry vector pDONR201 using the BP Clonase kit according to manufacturer's instructions (Invitrogen). The M_3 mAChR construct was subsequently transferred into the Gateway destination vector pEF5/FRT/V5-dest using the LR Clonase kit in accordance with the manufacturer's instructions (Invitrogen). The construct was then transfected into Flp-In CHO cells using methods described previously (Nawaratne et al., 2008). The same processes were applied to generate a vector containing the gene encoding the human $M_3K^{7.32}E$ (K523E) mAChR; however, before the BP Clonase reaction, a mutation was introduced using the QuikChange mutagenesis kit (Stratagene) by applying the oligonucleotides 5′-GTGACAGCTGCATACCCGAGACCTTTTGGAATCTGG-3′ and 5′-CCAGATTCCAAAAGGTCTCGGGTATGCAGCTGTCAC-3′ to the open vector, then following the manufacturer's instructions. Flp-In CHO cells stably expressing the M_3 mAChR (CHO M_3

mAChR cells) or the $M_3K^{7.32}E$ mAChR (CHO $M_3K^{7.32}E$ mAChR), were cultured at 37°C in 5% CO_2 in DMEM supplemented with 5% (v/v) FBS and 16 mM HEPES and were selected using 400 μg/ml hygromycin B but maintained using 200 μg/ml hygromycin B. For small interfering RNA (siRNA) experiments, cells were transfected with lipid alone, $G\alpha_q$ siRNA, or $G\alpha_{12}$ siRNA at a concentration of 100 nM per well (96-well format), using Lipofectamine 2000 according to the manufacturer's instructions.

Membrane Preparation. CHO M_3 mAChR (wild type) or $M_3K^{7.32}E$ mAChR cells were grown to 90% confluence, harvested, and centrifuged at 300*g* for 3 min. The intact cell pellet was suspended in homogenization buffer (20 mM HEPES, 10 mM EDTA, and 0.1 mg/ml saponin, pH 7.7) and further centrifuged (300*g*, 3 min). Cells were then resuspended in homogenization buffer and homogenized using a Polytron PT1200 homogenizer (Kinematica, Littau-Lucerne, Switzerland) for two 10-s intervals at maximum setting (6), with 30-s cooling periods on ice between each burst. The homogenate was then centrifuged (40,000*g*, 1 h, 4°C). The resulting pellet was resuspended in 5 ml of HEPES buffer (100 mM NaCl, 20 mM HEPES, and 10 mM $MgCl_2$, pH 7.4), and the protein content was determined using a bicinchoninic acid assay kit (Pierce Biotechnology, Rockford, IL) according to the manufacturer's instructions, using bovine serum albumin as a standard. The homogenate was then divided into 1-ml aliquots and either used immediately or stored frozen at −80°C until required.

Radioligand Binding Assays. Saturation and interaction binding assays were performed using 15 μg of membrane expressing the M_3 mAChR or $M_3K^{7.32}E$ mAChR receptors. For saturation binding assays, membranes were incubated with the orthosteric antagonist [^{3}H]NMS in HEPES buffer (20 mM HEPES, 100 mM NaCl, and 10 mM MgCl, pH 7.4) at 37°C for 1 h before termination of the assay by rapid filtration onto GF/B grade filter paper (Whatman, Maidstone, UK) using a Brandel harvester, followed by three 2-ml washes with ice-cold NaCl (0.9%). Nonspecific binding was defined in the presence of 10 μM atropine, and radioactivity was determined by liquid scintillation counting. For interaction binding studies, membranes were incubated in HEPES buffer containing 100 μM 2′/3′-*O*-(*N*-Methylanthraniloyl)guanosine-5′-[β,γ-imido]triphosphate with increasing concentrations of CCh in the absence or presence of brucine (3, 10, or 30 μM) and [^{3}H]NMS at a concentration equal to its equilibrium dissociation constant for each receptor (approximately 0.7 nM for both receptors) as determined from saturation binding experiments. Determination of nonspecific binding and termination of the experiment were as described above.

Ca^{2+} Mobilization Assay. CHO M_3 or $M_3K^{7.32}E$ mAChR cells were cultured overnight in 96-well plates at 37°C in 5% CO_2. Cells were washed twice in Ca^{2+} assay buffer (150 mM NaCl, 2.6 mM KCl, 1.2 mM $MgCl_2$, 10 mM dextrose, 10 mM HEPES, 2.2 mM $CaCl_2$, 0.5% (w/v) bovine serum albumin, and 4 mM probenecid), then replaced with Ca^{2+} assay buffer containing 1 μM Fluo-4-AM and incubated for 1 h at 37°C in 5% CO_2. Cells were washed twice more before replacement of the 37°C Ca^{2+} assay buffer. While fluorescence was measured, brucine was added for 1 min, CCh was subsequently added, and the response was measured further for 3 min in a Flexstation (Molecular Devices) using an excitation wavelength of 485 nm and an emission wavelength of 520 nm. Peak fluorescence was measured as a marker for Ca^{2+} mobilization and used in further analyses.

Cytoskeletal Rearrangement Assay and Image Analysis. CHO M_3 and $M_3K^{7.32}E$ mAChR cells were cultured overnight in 96-well plates at 37°C in 5% CO_2. Samples were serum-starved 4 h before assaying and then treated with ligand at time points as follows: CCh, 2 min; brucine, 15 min (determined by separate time course assays). The assays were terminated, fixed, stained, and analyzed as described by Stewart et al. (2010). In brief, samples were fixed in 4% paraformaldehyde and permeabilized in 0.3% (v/v) Tween 20 in phosphate-buffered saline. Samples were stained with 0.2 μg/ml Hoechst 33342 and 2 U/mL Alexa Fluor 568-phalloidin and imaged using an IN Cell analyzer 1000 (GE Healthcare, Chalfont St. Giles, Buckinghamshire, UK). For the cytoskeletal analysis component, the images were randomized and blinded and then analyzed manually to detect the number of cells that exhibited membrane ruffling. That number was subsequently normalized to the nuclei content per image, which were counted using IN Cell Developer software. Each data point on the concentration-response curve represents one image performed in duplicate over the number of times indicated in the figure legends. On average, approximately 200 cells were present in each image.

Extracellular Signal-Regulated Kinase 1/2 Phosphorylation Assays. Initial ERK1/2 phosphorylation time course experiments were performed to determine the time at which ERK1/2 phosphorylation was maximal after stimulation by each agonist at a single concentration, in addition to coadministration of brucine (10 μM) with CCh (1 μM). Cells were seeded into transparent 96-well plates at 5×10^4 cells per well and grown overnight. The cells were then washed twice with phosphate-buffered saline and incubated in serum-free DMEM at 37°C for at least 4 h. For interaction studies between CCh and brucine, cells were then stimulated with brucine for 1 min before CCh stimulation for 5 min and incubated at 37°C in 5% CO_2. For experiments in which PTX pretreatment was required, cells were treated with 100 ng/ml PTX in serum-free DMEM overnight. For all experiments, 10% (v/v) FBS was used as a positive control, and vehicle controls were also performed. The reaction was terminated by removal of media and drugs, and the cells were then lysed with 100 μl of *SureFire* lysis buffer (as provided by the manufacturer). The lysates were agitated for 1 to 2 min and were diluted at a ratio of 4:1 (v/v) lysate/*Surefire* activation buffer in a total volume of 50 μl. Under low light conditions, a 1:240 (v/v) dilution of AlphaScreen beads:Surefire reaction buffer was prepared, and this was mixed with the activated lysate mixture in a ratio of 6:5 (v/v), respectively, in a 384-well opaque Optiplate. Plates were incubated in the dark at 37°C for 1 h before the fluorescence signal was measured using a Fusion-α plate reader (PerkinElmer Life and Analytical Sciences) using standard AlphaScreen settings. Data were normalized to the maximal response elicited by 10% (v/v) FBS at the same time point.

Data Analysis. All data were analyzed using Prism 5.02 (GraphPad Software, San Diego, CA). For radioligand saturation binding data, nonspecific and total binding data were fitted to the following equation:

$$Y = \frac{B_{max} \cdot [A]}{[A] + K_A} + NS \cdot [A] \quad (1)$$

where Y is radioligand binding, B_{max} is the total receptor density, [A] is the radioligand concentration, K_A is the equilibrium dissociation constant of the radioligand, and NS is the fraction of nonspecific radioligand binding. For interaction binding experiments, the shifts of the carbachol versus [^{3}H]NMS competition binding curves obtained in the absence or presence of brucine were fitted to the following allosteric binding model (Christopoulos, 2000):

$$Y = \frac{B_{max} \cdot [A]}{[A] + K_{App}} \quad (2)$$

where

$$K_{App} = \frac{K_A \cdot K_B}{\alpha \cdot [B] + K_B} \cdot \left[1 + \frac{[I]}{K_I} + \frac{[B]}{K_B} + \frac{\alpha' \cdot [I] \cdot [B]}{K_I \cdot K_B}\right] \quad (3)$$

and [I] denotes the concentration of (orthosteric) competitor; [B] denotes the concentration of allosteric modulator; K_A, K_B, and K_I denote the equilibrium dissociation constants of the radioligand, modulator, and competitor, respectively; α denotes the modulator-radioligand binding cooperativity factor, which is a measure of the magnitude and direction of the allosteric effect the modulator exerts on the affinity of radioligand; and α' defines the binding cooperativ-

ity factor between the allosteric ligand and orthosteric competitor. Values of α or $\alpha' > 1$ denote positive cooperativity, values < 1 (but greater than 0) denote negative cooperativity, values $= 1$ denote neutral cooperativity, and values approaching zero denote inhibition that is indistinguishable from competitive (orthosteric) antagonism.

For some experiments (see *Results*), concentration-response data generated from functional assays were fitted to the following logistic equation:

$$E = \text{Basal} + \frac{E_{max} - \text{basal}}{1 + 10^{(-\text{pEC}_{50} - \text{Log[A]} - \text{Log}\delta)}} \quad (4)$$

where E is effect; E_{max} and basal are the top and bottom asymptotes of the curve, respectively; Log[A] is the logarithm of the agonist concentration; pEC_{50} is the negative logarithm of the agonist concentration that gives a response halfway between E_{max} and basal (i.e., $-$ve $LogEC_{50}$) in the absence of allosteric modulator; and Logδ is the logarithm of the difference between the EC_{50} of an agonist in the presence of a maximal concentration of allosteric modulator to that determined in the absence of modulator (see *Results*); the determination of Logδ as a directly fitted parameter, rather than as a calculated ratio of two separately derived EC_{50} values, facilitated the statistical comparison of agonist curve shifts in the presence of modulator among various treatment groups (see *Results*).

Data from functional experiments measuring the interaction between CCh and brucine at the M_3 and $M_3K^{7.32}E$ mAChR were also fitted to the following operational model for the interaction between a full orthosteric agonist and an allosteric modulator (Leach et al., 2010):

$$E = \text{Basal} + \frac{(E_m - \text{Basal})([A](K_B + \alpha\beta[B]) + \tau_B[B][EC_{50}])}{[EC_{50}](K_B + [B]) + ([A](K_B + \alpha\beta[B]) + \tau_B[B][EC_{50}])} \quad (5)$$

where E denotes the effect, A denotes the agonist, B denotes the allosteric modulator, $\alpha\beta$ denotes a composite cooperativity factor that quantifies the change in affinity (α) and signaling efficacy (β) imparted to the receptor by the agonist as a result of the presence of allosteric modulator, E_m denotes the maximal response of the system, EC_{50} is the agonist concentration that gives a response halfway between E_m and basal, K_B is the equilibrium dissociation constant for the modulator, and [A] is the radioligand concentration. The key advantage of the operational model is in its ability to be directly fitted to experimental data to derive parameter estimates of allosteric modulator and agonist effects. However, it should also be noted that the model is mechanistically limited in that it cannot derive parameters that describe the molecular properties underlying agonism and allosteric modulation of signaling efficacy; the resulting parameters are composite values that also reflect the influence of receptor density and stimulus-response coupling on the observed responses.

All parametric measures of potency, affinity, operational efficacy, and cooperativity were estimated as logarithms (Christopoulos,

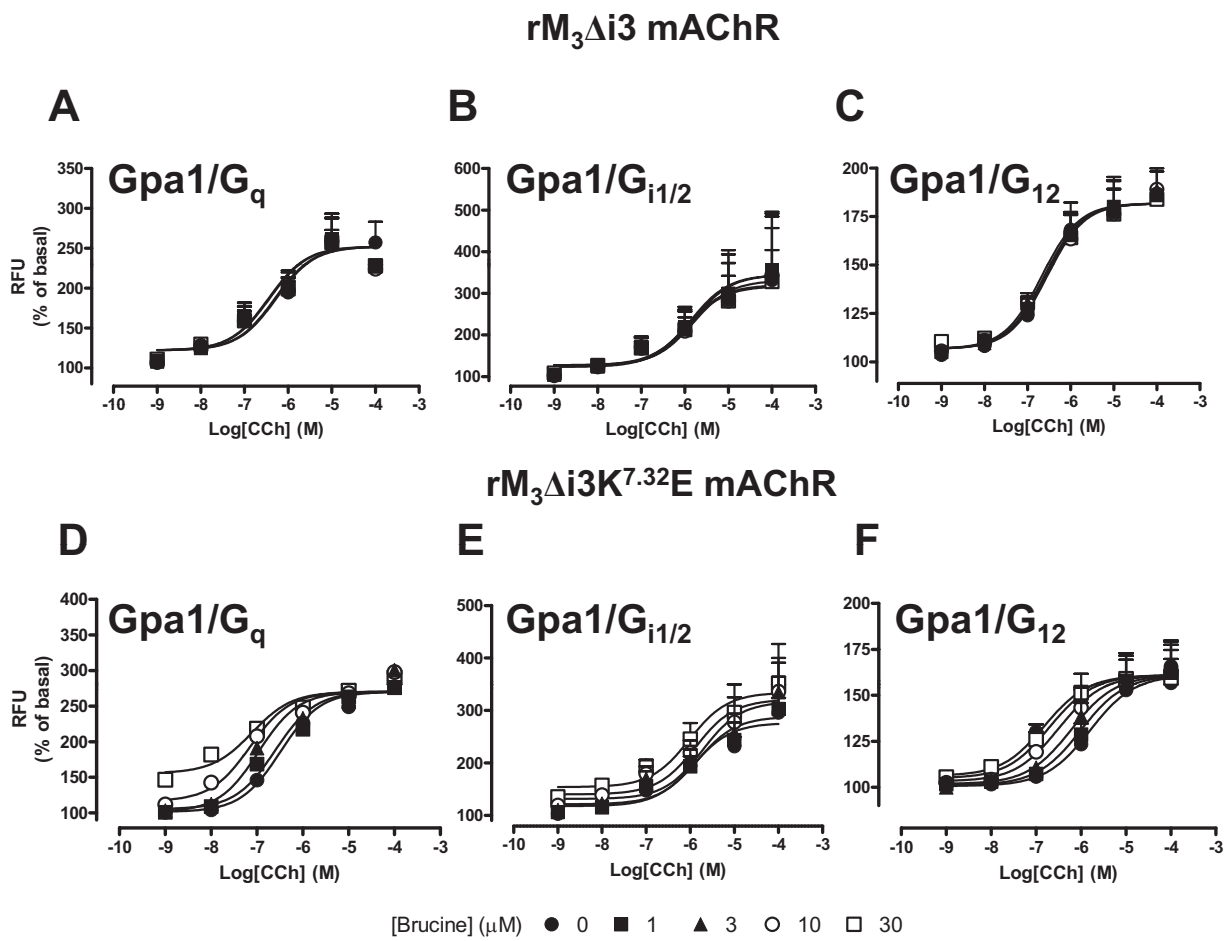

Fig. 1. Effects of brucine on CCh concentration-response curves in yeast. CCh concentration-response curves were determined in yeast strains expressing the $rM_3\Delta i3$ mAChR and Gpa1/$G\alpha_q$ (A), Gpa1/$G\alpha_{i1/2}$ (B), or Gpa1/$G\alpha_{12}$ (C) or in yeast strains expressing the $rM_3\Delta i3K^{7.32}E$ mAChR and Gpa1/$G\alpha_q$ (D), Gpa1/$G\alpha_{i1/2}$ (E), or Gpa1/$G\alpha_{12}$ (F) in the absence and presence of brucine. Data points are expressed as mean percentage of the basal activity in the absence of brucine + S.E.M. obtained from three to five experiments performed in duplicate. RFU, relative fluorescence units.

1998). Statistical comparisons between parameters were performed using a Student's t test or one-way ANOVA with a Newman-Keul's multiple comparison post test, as appropriate, and $p < 0.05$ taken as indicating significance.

Results

Effect of Brucine on Carbachol Signaling at the $rM_3\Delta i3$ and $rM_3\Delta i3K^{7.32}E$ mAChR in Yeast. Previous studies have demonstrated that the introduction of a third intracellular loop deletion into the rat M_3 mAChR ($rM_3\Delta i3$ mAChR) yields a construct that displays robust cell-surface expression in yeast but retains pharmacological characteristics of the wild-type receptor (Erlenbach et al., 2001). Therefore, this mutant receptor was used for all our studies in the *S. cerevisiae* strains reported herein. To ascertain whether allosteric modulation could be detected in yeast signaling assays, interaction studies were performed between CCh and brucine at the $rM_3\Delta i3$ and $rM_3\Delta i3K^{7.32}E$ mAChR in yeast strains expressing Gpa1/Gα_q, Gpa1/Gα_{12}, or Gpa1/G$\alpha_{i1/2}$ (Fig. 1). In all yeast strains expressing the $rM_3\Delta i3$ mAChR, brucine had no appreciable effect on the carbachol concentration-response curve. However, in strains expressing the $rM_3\Delta i3K^{7.32}E$ mAChR, brucine exhibited differential effects on carbachol signaling in a G protein-dependent manner. Specifically, brucine displayed both agonism and potentiation of the carbachol response when coupled to Gpa1/Gα_q, whereas it displayed no agonism but a robust sinistral shift of the carbachol concentration-response curve when coupled to Gpa1/Gα_{12}. When the $rM_3\Delta i3K^{7.32}E$ mAChR was coupled to Gpa1/G$\alpha_{i1/2}$, brucine had no effect on carbachol responsiveness. In addition, from the data in yeast expressing the $rM_3\Delta i3K^{7.32}E$ mAChR and Gpa/Gα_q or Gpa/Gα_{12}, we derived brucine affinity (Log K_B), efficacy (Log τ_B) and cooperativity (Log $\alpha\beta$) estimates using eq. 5 (Table 1).

Differential Effects of Brucine on Carbachol and [^{3}H]NMS Binding at Human M_3 and $M_3K^{7.32}E$ mAChRs in Mammalian Cell Membranes. Radioligand saturation binding studies were performed on CHO cell membranes expressing either the full-length M_3 wild type or $M_3K^{7.32}E$ mAChR, from which B_{max} and [^{3}H]NMS affinity values were derived using eq. 1 (Table 2). These studies revealed that there was no difference between the affinity of [^{3}H]NMS for each receptor and that receptor expression did not change between cell lines. Interaction binding studies were also performed between [^{3}H]NMS, CCh, and brucine to determine the effect of brucine on the affinity of the radioligand and the nonradiolabeled orthosteric competitor (Fig. 2). From these data, brucine affinity and cooperativity values were derived

TABLE 1

Operational model parameters for the interaction between CCh and brucine at the $rM_3\Delta i3K^{7.32}E$ mAChR in yeast

Data are expressed as the mean ± S.E.M. of three to five separate experiments performed in duplicate.

	Gpa1/Gα_q	Gpa1/Gα_{12}
Log K_B	−4.48 ± 0.13	−4.89 ± 0.13
Log τ_B	0.15 ± 0.07 (τ_B = 1.4)	−0.79 ± 0.17** (τ_B = 0.16)
Log $\alpha\beta$	0.76 ± 0.17 ($\alpha\beta$ = 5.8)	1.06 ± 0.10 ($\alpha\beta$ = 11.5)

Log K_B, logarithm of the dissociation constant of the allosteric modulator; Log τ_B, logarithm of the operational efficacy of the allosteric modulator; Log $\alpha\beta$, logarithm of the cooperativity of the allosteric modulator on the potency of the orthosteric agonist.

** $P < 0.01$ determined by Student's t test (compared with the same parameter in the Gpa1/Gα_q strain).

TABLE 2

Saturation binding parameters for [^{3}H]NMS at the M_3 or $M_3K^{7.32}E$ mAChR in CHO cell membranes

Data are presented as the mean ± S.E.M. of three separate experiments performed in duplicate.

	CHO M_3 mAChR	CHO $M_3K^{7.32}E$ mAChR
Log K_A[a]	−9.14 ± 0.05	−9.20 ± 0.04
B_{max} (fmol/mg protein)[b]	3425 ± 233	2940 ± 338

Log K_A, logarithm of the equilibrium dissociation constant of the radioligand; B_{max}, total number of binding sites, determined by specific binding of the radioligand.

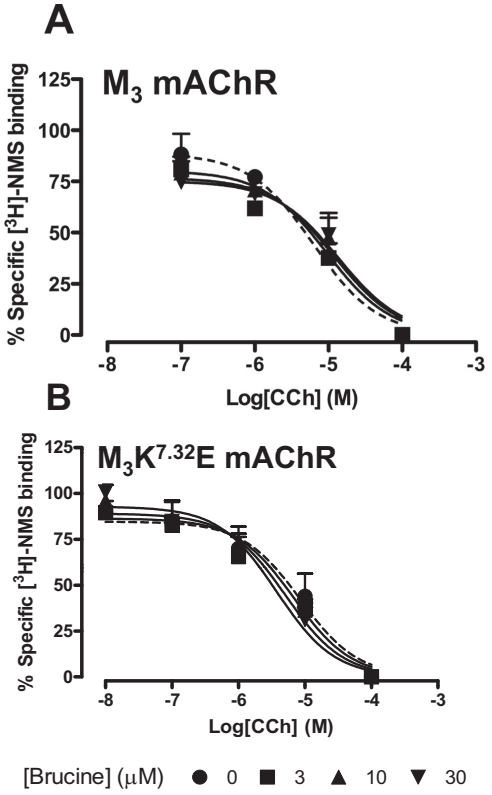

Fig. 2. The allosteric modulator brucine displays differential cooperativity at the M_3 and $M_3K^{7.32}E$ mACh receptors. Interaction between [^{3}H]NMS and carbachol at the M_3 (A) or $M_3K^{7.32}E$ mAChR (B) in the absence and presence of brucine. Dashed lines represent the curve fit for the CCh inhibition curve in the absence of brucine. Data points are represented as the mean percentage of specific [^{3}H]NMS binding in the absence of CCh or brucine + S.E.M. of three experiments performed in duplicate.

TABLE 3

Allosteric ternary complex model binding parameters for the interaction between [^{3}H]NMS, CCh, and brucine at the M_3 and $M_3K^{7.32}E$ mAChRs in CHO cell membranes

Data are presented as the mean ± S.E.M. of three separate experiments performed in duplicate.

	CHO M_3 mAChR	CHO $M_3K^{7.32}E$ mAChR
Log K_B	−5.95 ± 0.37	−5.06 ± 0.15
Log K_I	−5.48 ± 0.03	−5.32 ± 0.04*
Log α	−0.12 ± 0.03 (α = 0.75)	0.10 ± 0.03** (α = 1.25)
Log α'	−0.35 ± 0.26 (α' = 0.45)	0.58 ± 0.04* (α' = 3.80)

Log K_B, logarithm of the dissociation constant of the allosteric modulator; Log K_I, logarithm of the dissociation constant of the orthosteric inhibitor; Log α, logarithm of the cooperativity between the allosteric modulator on the radioligand; Log α', logarithm of the cooperativity between the allosteric modulator on the orthosteric inhibitor.

* $P < 0.05$ determined by Student's t test (compared with the same parameter at the CHO M_3 mAChR).

** $P < 0.01$ determined by Student's t test (compared with the same parameter at the CHO M_3 mAChR).

using eq. 2 (Table 3). Affinity values for [^{3}H]NMS, CCh, and brucine derived from the binding assays were similar across the M_3 and $M_3K^{7.32}E$ mAChRs, suggesting that the mutation had little effect on the orthosteric or allosteric ligand binding pockets. It is noteworthy, however, that the modulatory effect of brucine on orthosteric ligand binding was altered by the $K^{7.32}E$ mutation, because brucine displayed slight negative cooperativity for [^{3}H]NMS and CCh binding at the M_3 mAChR but modest positive cooperativity at the $M_3K^{7.32}E$ mAChR.

Validation of Brucine Pharmacology in Mammalian Cells Expressing the Human M_3 and $M_3K^{7.32}E$ mAChR. Data generated in the yeast assays suggested that brucine had no effect on CCh signaling at the $rM_3\Delta i3$ mAChR, but exhibited agonism in the Gpa/Gα_q yeast strain and robust potentiation of CCh function in the Gpa/Gα_{12} strain at the $rM_3\Delta i3K^{7.32}E$ mAChR. To ascertain whether these findings were relevant to a mammalian cell background, experiments were performed in CHO cells expressing either the human M_3 or $M_3K^{7.32}E$ mAChR using Ca^{2+} mobilization and membrane ruffling as surrogate assays for G_q and G_{12}, respectively (Brown et al., 2006; Ridley, 2006; Yuan et al., 2006).

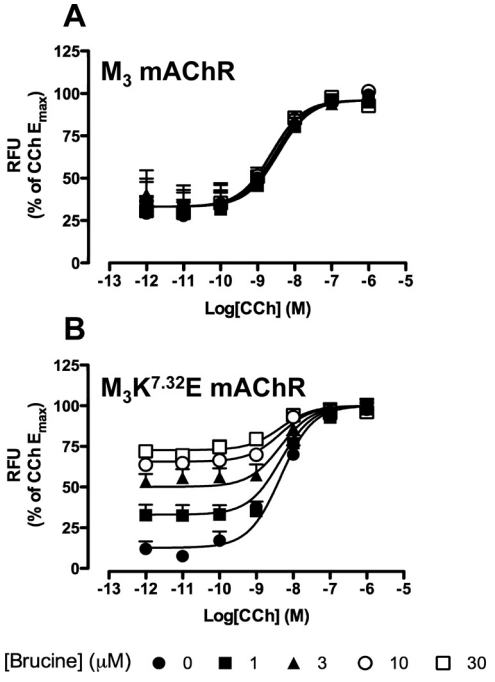

Fig. 3. Effect of brucine on CCh-induced Ca^{2+} mobilization in CHO cells. CCh concentration-response curves performed in CHO cells expressing the M_3 (A) or the $M_3K^{7.32}E$ (B) mAChR in the absence and presence of brucine. Data points are expressed as mean percentage of the maximal CCh-induced Ca^{2+} mobilization response in the absence of brucine + S.E.M. obtained from four to six experiments performed in duplicate.

Interaction studies were initially performed in CHO cells expressing the M_3 or $M_3K^{7.32}E$ mAChR, with Ca^{2+} mobilization as a functional endpoint (Fig. 3). As observed in Gpa1/Gα_q yeast strains expressing the $rM_3\Delta i3$ mAChR, brucine had no effect on the CCh concentration-response curve in CHO cells expressing the M_3 mAChR. However, brucine exhibited both agonism and potentiation of the CCh concentration-response curve in CHO cells expressing the $M_3K^{7.32}E$ mAChR. Application of eq. 5 to the $M_3K^{7.32}E$ mAChR data yielded the operational model parameter estimates shown in Table 4.

Subsequent time course studies in CHO M_3 and $M_3K^{7.32}E$ mAChR cells revealed that the CCh-induced membrane ruffling response peaked at 2 min and that brucine did not alter the time-course profile of CCh or exhibit agonism for this pathway in either cell line (data not shown). CCh concentration-response curves were then constructed in the absence and presence of brucine in membrane ruffling assays in CHO cells expressing the M_3 or $M_3K^{7.32}E$ mAChR (Figs. 4 and 5). The results were consistent with those found in the yeast signaling assay for Gpa1/Gα_{12} coupling, in which brucine had no effect on the CCh concentration-response curves at the $rM_3\Delta i3$ mAChR but was able to robustly potentiate CCh-induced signaling at the $rM_3\Delta i3K^{7.32}E$ mAChR without displaying any allosteric agonism. Table 4 shows the Log K_B, Log $\alpha\beta$, and Log τ_B values that were derived by applying eq. 5 to the $M_3K^{7.32}E$ mAChR data from membrane ruffling assays.

Use of Modulator Profiling in Yeast to Delineate Possible Modes of Convergent Pathway Signaling at the $M_3K^{7.32}E$ mAChR. In conjunction with generating a G protein profile for receptor-ligand interaction, we reasoned that another possible utility of pairing the yeast signaling assay with a functionally selective modulator could be to aid in the dissection of intracellular G protein mediators of a convergent signaling pathway. For the purposes of the current study, we chose the phosphorylation of ERK1/2 as one such pathway (Werry et al., 2006). Specifically, the profile of the effect of brucine at different G protein subtypes may be used to predict which G protein (if any) underlies the predominant mode of coupling that leads to $M_3K^{7.32}E$ mAChR-mediated phosphorylation of ERK1/2. Therefore, the effect of brucine on ERK1/2 phosphorylation was investigated. Time-course studies were performed in CHO M_3 and $M_3K^{7.32}E$ mAChR cells, which demonstrated that maximal CCh-induced ERK1/2 phosphorylation occurred approximately 5 min after stimulation (data not shown). From this, it was also noted that brucine did not display agonism and did not alter the time point of the peak CCh response. Interaction studies between carbachol and brucine at M_3 and $M_3K^{7.32}E$ mAChRs were then performed to determine the effect of brucine on the potency of CCh at both receptors (Fig. 6). The results revealed

TABLE 4

Operational model parameters for the interaction between CCh and brucine at the $M_3K^{7.32}E$ mAChR

Data are presented as the mean ± S.E.M. of three to six separate experiments performed in duplicate.

	Ca^{2+} Mobilization	Membrane Ruffling	ERK1/2 Phosphorylation	ERK1/2 Phosphorylation + PTX
Log K_B	−5.17 ± 0.15	−4.61 ± 0.13	−5.21 ± 0.28	−5.30 ± 0.19
Log τ_B	0.41 ± 0.03** (τ_B = 2.6)	−1.40 ± 0.48 (τ_B = 0.04)	−0.66 ± 0.16 (τ_B = 0.2)	−0.43 ± 0.16 (τ_B = 0.4)
Log $\alpha\beta$	0.70 ± 0.17 ($\alpha\beta$ = 5.0)	0.88 ± 0.10 ($\alpha\beta$ = 7.6)	0.84 ± 0.06 ($\alpha\beta$ = 6.9)	0.84 ± 0.07 ($\alpha\beta$ = 6.9)

Log K_B, logarithm of the dissociation constant of the allosteric modulator; Log τ_B, logarithm of the operational efficacy of the allosteric modulator; Log $\alpha\beta$, logarithm of the cooperativity of the allosteric modulator on the potency of the orthosteric agonist.

** $P < 0.01$ determined by one-way ANOVA with Newman-Keuls multiple comparisons post test across Log τ_B values (statistically different to the Log τ_B value derived for membrane ruffling).

that brucine had little effect on CCh concentration-response curves from CHO M_3 mAChR cells, whereas brucine potentiated the CCh response at the $M_3K^{7.32}E$ mAChR in a concentration-dependent manner. If ERK1/2 phosphorylation was downstream of G protein coupling, then the lack of agonism displayed by brucine suggested an absence of G_q contribution to M_3 mAChR-mediated ERK1/2 phosphorylation. Moreover, the yeast assays also predicted no coupling to $G_{i/o}$ proteins. To confirm the latter, the same ERK1/2 phosphorylation assays were performed in the presence of PTX pretreatment (Fig. 6). The lack of effect of PTX on $M_3K^{7.32}E$ mAChR-mediated ERK1/2 phosphorylation suggested that $G_{i/o}$ proteins had no contribution to this pathway, as predicted. Table 4 shows operational model parameter estimates derived by applying eq. 5 to the ERK1/2 phosphorylation data from studies at the $M_3K^{7.32}E$ mAChR in the absence and presence of PTX.

Given the absence of contribution by G_q and $G_{i/o}$ proteins to the allosteric modulation by brucine of $M_3K^{7.32}E$ mAChR-mediated ERK1/2 phosphorylation, we speculated that this allosteric effect is potentially mediated selectively via G_{12} activation converging into the ERK1/2 stimulus-response chain. To more directly examine this hypothesis, we determined the effects of 30 μM brucine on CCh-mediated signaling in mammalian cells in the absence and presence of siRNA directed against mRNA of $G\alpha_q$ or $G\alpha_{12}$ (Fig. 7). Although the degree of direct allosteric agonism mediated by brucine itself in Ca^{2+} mobilization assays was reduced by the presence of transfection lipid, robust potentiation of CCh-mediated signaling was still evident in the absence of siRNA (Fig. 7A), as well as in the presence of $G\alpha_{12}$ siRNA (Fig. 7C), but was significantly attenuated upon transfection of $G\alpha_q$ siRNA (Fig. 7B; Table 5), as expected. In contrast, selective knockdown of $G\alpha_q$ had minimal effect on the capacity of brucine to potentiate the CCh-stimulated ERK1/2 phosphorylation (Fig. 7, D and E), whereas knockdown of $G\alpha_{12}$ virtually abolished the allosteric potentiation (Fig. 7F; Table 5), consistent with a selective role of $G\alpha_{12}$ activation in mediating the allosteric modulation of the ERK1/2 response.

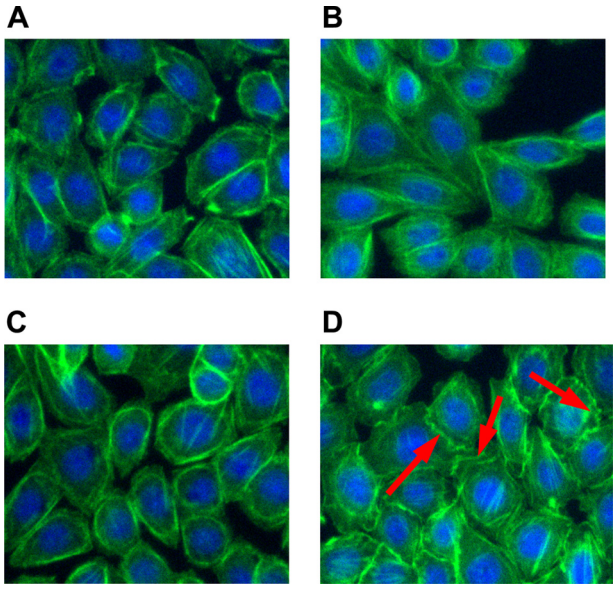

Fig. 4. Representative images of membrane ruffling in CHO $M_3K^{7.32}E$ mAChR cells. CHO $M_3K^{7.32}E$ mAChR cells fixed in paraformaldehyde and stained with Alexa-568-conjugated phalloidin (green) and Hoechst 33342 nuclear dye (blue), post treatment with serum-free DMEM (A), 1 μM CCh (B), 100 μM brucine (C), or 1 μM CCh + 100 μM brucine (D). Red arrows indicate regions of cell membranes that are ruffled.

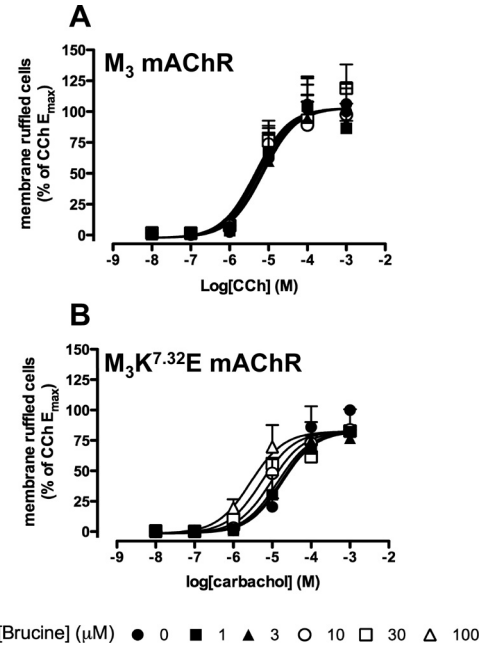

Fig. 5. Effect of brucine of carbachol-induced membrane ruffling in CHO cells. Carbachol concentration-response curves performed in CHO cells expressing the M_3 (A) or the $M_3K^{7.32}E$ (B) mAChR in the absence and presence of brucine. Data points are presented as mean percentage of the maximal CCh-induced membrane ruffling response in the absence of brucine + S.E.M. obtained from three experiments performed in duplicate.

Discussion

To our knowledge, this study is the first to use the yeast system to detect functional selectivity of an allosteric ligand and to show that brucine is capable of exhibiting pathway selectivity. Furthermore, using the yeast system and the unique properties of brucine at the $K^{7.32}E$ mutant as pharmacological tools allowed us to determine a putative G protein candidate for brucine biased modulation of $M_3K^{7.32}E$ mAChR-mediated ERK1/2 phosphorylation pathway in mammalian (CHO) cells.

Numerous studies have investigated the properties of allosteric ligands that bind at mAChRs (Gregory et al., 2007), the majority focusing on ligands that bind to the "prototypical" binding site. Indeed, mutagenesis studies have mapped extracellular regions of mAChRs to determine amino acids residues that are pivotal for allosteric binding of the prototypical modulator, gallamine, and associated ligands (Gnagey et al., 1999; Buller et al., 2002). However, most of these studies focused on the effects of mutagenesis on radioligand binding or used only a single signaling endpoint to define functional pharmacology (e.g., Jakubík et al., 1996; Iarriccio, 2008). In contrast, our current study investigated the ability of brucine to engender functional selectivity at the $M_3K^{7.32}E$ mAChR by adopting the use of the yeast signaling assay as a predictive screen in conjunction with a multiplatform approach for mammalian system validation. The results produced in all of the yeast strains expressing the $rM_3\Delta i3$ mAChR showed that brucine had no effect on CCh signaling, which was con-

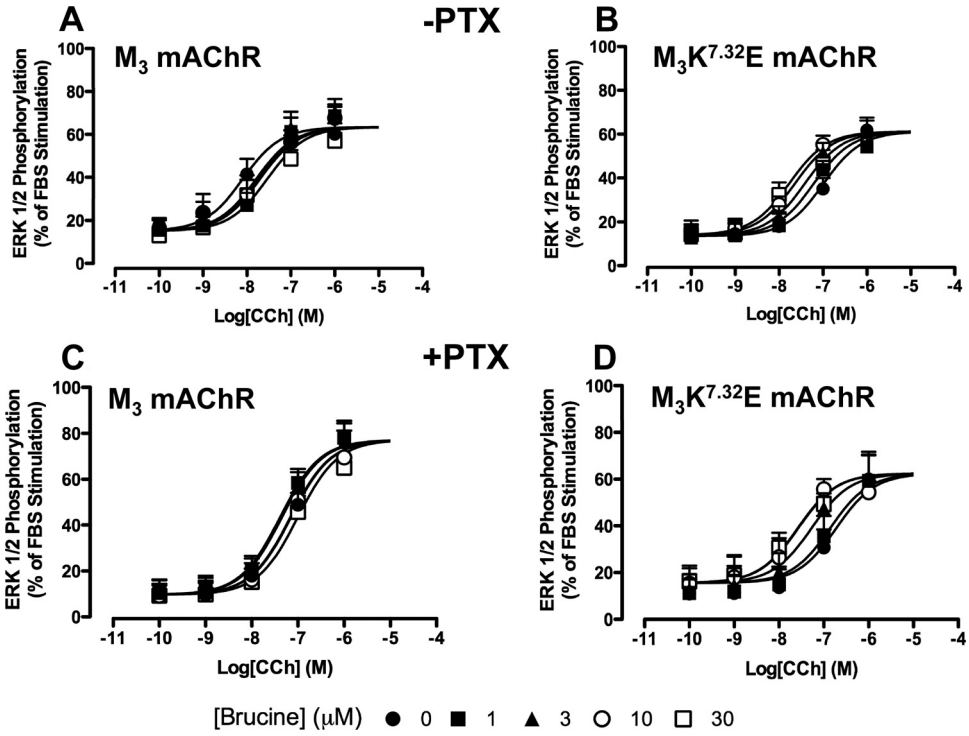

Fig. 6. Effect of brucine on CCh-induced ERK1/2 phosphorylation in CHO cells. CCh concentration-response curves performed in CHO cells expressing the M_3 (A) or the $M_3K^{7.32}E$ (B) mAChR in the absence and presence of brucine. These experiments were also performed after preincubation with PTX at the M_3 (C) and $M_3K^{7.32}E$ (D) mAChR. Data points are represented as mean percentage of the peak ERK1/2 phosphorylation response elicited by 10% FBS + S.E.M. obtained from three to six experiments performed in duplicate.

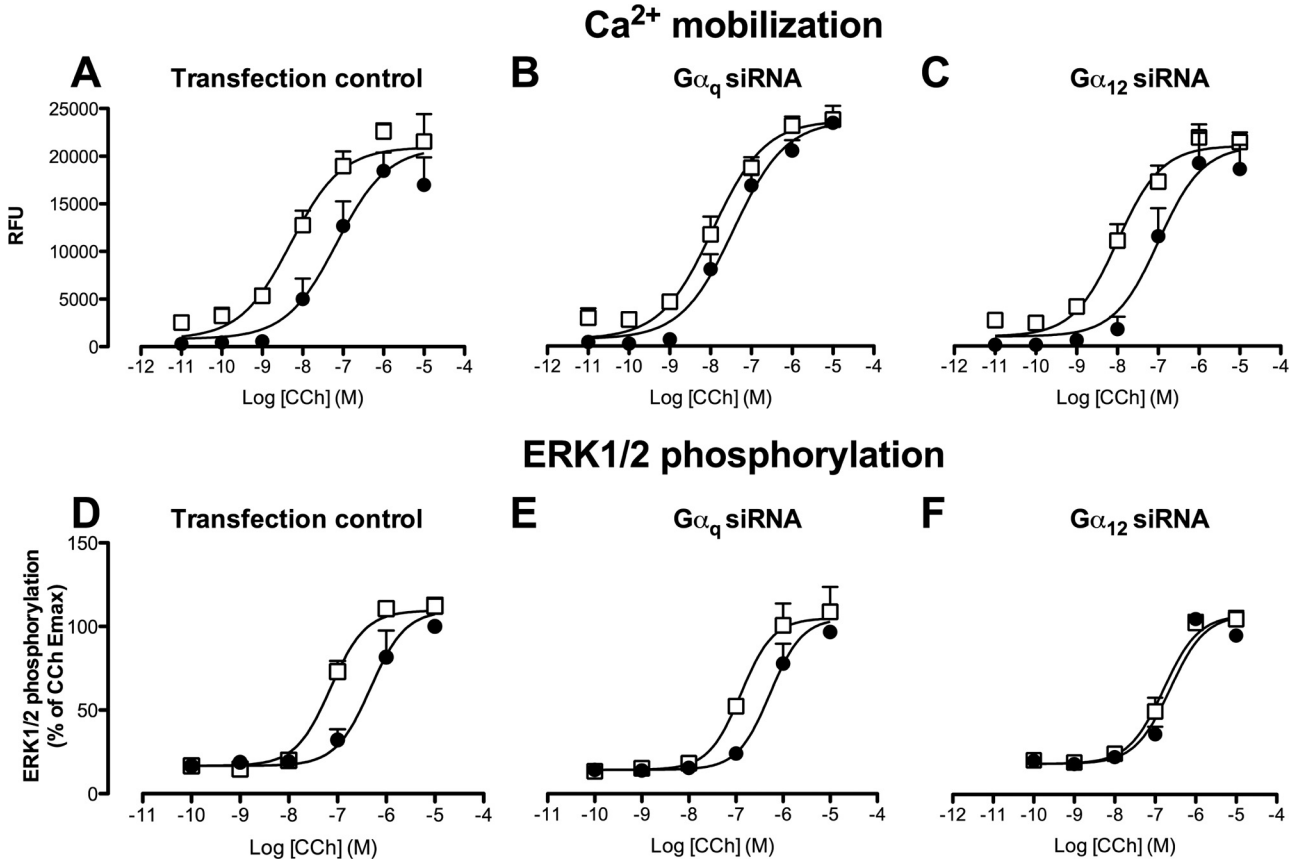

Fig. 7. Impact of G protein-targeting siRNA on the ability of brucine to allosterically potentiate the CCh-stimulated response. CCh concentration-response curves performed in CHO $M_3K^{7.32}E$ mAChR cells, in the absence (●) or presence (□) of 30 μM brucine, in Ca^{2+} mobilization (A, B, and C) and ERK1/2 phosphorylation assays (D, E, and F). Experiments were conducted 48 h after transfection with transfection lipid alone (transfection control), $G\alpha_q$ siRNA, or $G\alpha_{12}$ siRNA. Data are expressed as the mean RFU (Ca^{2+}mobilization) or ERK1/2 phosphorylation as a percentage of the peak CCh response from the control data (ERK1/2 phosphorylation) + S.E.M. collected from four experiments performed in duplicate.

firmed in CHO M_3 mAChR cells. This result is consistent with what was found by Iarriccio (2008). The data generated from the yeast signaling assays at the $K^{7.32}E$ mutant, however, suggested that brucine was an agonist with modest enhancement of CCh signaling when coupled to G_q-mediated pathways. These data are concordant with those generated for CCh-induced Ca^{2+} signaling in CHO $M_3K^{7.32}E$ mAChR cells and also indicate that the use of a truncated rat receptor in yeast did not lead to spurious findings that could not be validated at the full-length human receptor in mammalian cells. In both assay types, brucine induced a progressive sinistral shift of the CCh concentration-response curve of approximately 0.5 Log units as well as displaying its own agonism. The degree of brucine agonism varied between the yeast and CHO cell assays, as quantified by the operational model parameters, $\tau_B = 1.4$ and 2.6, respectively, which may be due to a lower receptor expression in the yeast system compared with CHO $M_3K^{7.32}E$ mAChR cells.

Interaction binding assays between CCh and brucine in membranes expressing the M_3 and $M_3K^{7.32}E$ mAChR demonstrated that the $K^{7.32}E$ mutation did not greatly affect the binding of [^{3}H]NMS, CCh, or brucine but rather weakly enhanced the cooperativity of brucine with the orthosteric ligands. These binding cooperativity profiles are consistent with the recent study by Iarriccio (2008), and the almost neutral cooperativity exhibited by brucine at wild-type M_3 mAChR is also consistent with evidence from previous studies at the same receptor (Lazareno et al., 1998). However, despite the cooperativities being similar, there was a discrepancy between the affinity estimates of brucine at the unoccupied M_3 mAChR from binding studies (Table 3), compared with the values derived by Iarriccio (2008); Log $K_B = -3.89$) and Lazareno et al. (1998); Log $K_B = -3.52$); this may be due to different assay conditions.

It is noteworthy that interaction studies between CCh and brucine at the $rM_3\Delta i3K^{7.32}E$ in the Gpa1/$G\alpha_{12}$ yeast strain were able to predict the functional profile of brucine in membrane ruffling in CHO $M_3K^{7.32}E$ mAChR cells, where brucine treatment resulted in a concentration-dependent sinistral shift of the CCh concentration-response curve. Unlike G_q signaling, brucine did not display agonism, suggesting that the modulator is a selective (direct) allosteric agonist for G_q-coupling at the mutant receptor but a selective positive allosteric modulator for G_{12}-mediated CCh signaling. There was a good accord in the rank order of $\alpha\beta$ and τ values derived from yeast G protein assays and their surrogate CHO cell assay, suggesting that the yeast assay is predictive of allosteric ligand pharmacology in mammalian cells.

As mentioned previously, numerous studies have investigated mAChR allosteric binding site mutations and allosteric ligand pharmacology, but with one exception (Leach et al., 2010), these studies have not generally probed for evidence of functional selectivity. However, given a surge in findings of functional selectivity induced by orthosteric ligands at various GPCRs (Baker et al., 2003; Galandrin et al., 2008), some evidence that allosteric ligands may also induce pathway-selective signaling has recently emerged at other GPCRs. For example, prostaglandin D_2 receptor-mediated phosphoinositide signaling is not affected by the allosteric ligands 1-(4-ethoxyphenyl)-5-methoxy-2-methylindole-3-carboxylic acid and N_α-tosyltryptophan, but both abrogate prostaglandin D_2 receptor-mediated arrestin recruitment via a non–G protein-dependent mechanism (Mathiesen et al., 2005). Likewise, the allosteric ligand LPI805 was able to potentiate NKA-induced Ca^{2+} mobilization while allosterically inhibiting NKA-induced cAMP accumulation at the tachykinin NK_2 receptor (Maillet et al., 2007). Thus it should not be surprising that this phenomenon may occur at other pleiotropically coupled receptors, such as the M_3 mAChR.

Given that the purpose of the current study was predominantly to provide proof of concept in the utility of pairing a yeast screening assay with a functionally selective allosteric ligand, we also attempted to ascertain whether this pairing can provide insights into a convergent signaling pathway, in essence, to perform a ligand-dependent G protein "fingerprint" for likely candidates coupling the $M_3K^{7.32}E$ mAChR to ERK1/2 phosphorylation. In yeast, brucine was a selective agonist for Gpa1/$G\alpha_q$ coupling, and the fact that brucine alone did not elicit an ERK1/2 phosphorylation response suggests a lack of involvement of G_q $M_3K^{7.32}E$ mAChR-mediated ERK1/2 phosphorylation in CHO cells. The pretreatment of CHO $M_3K^{7.32}E$ mAChR cells with PTX did not affect the potency of CCh or cooperativity of brucine, implying a lack of $G_{i/o}$-mediated signaling, as predicted by the yeast assay. It is noteworthy that the knockdown of $G\alpha_q$ or $G\alpha_{12}$ proteins did not diminish the potency of CCh, indicating that $M_3K^{7.32}E$ mAChR-mediated ERK1/2 activation by this orthosteric agonist involves additional (e.g., G protein-independent) components and/or that the degree of knockdown was insufficient to overcome the high efficacy of the agonist for receptor activation. However, the abolishment of brucine's allosteric effect on the CCh response in ERK1/2 phosphorylation assays by $G\alpha_{12}$ siRNA clearly indicated that the allosteric modulator can promote a unique conformation that recruits $G\alpha_{12}$ to converge on receptor coupling to the ERK1/2-response, further validating the use of the yeast assay as a predictor of this novel property.

Results from this study also suggest that residue 7.32 is not necessarily vital for either orthosteric ligand or brucine binding; instead, it may be an important region for maintaining the flexibility, and hence possibly activation, of the receptor. Although the finer points of GPCR activation are still largely unknown, there is evidence that some residues in TMVII can form intramolecular interactions with residues in TMIII, to increase the stability of the receptor in an inactive state in the angiotensin II type 1 receptor and opsin, suggesting that TMVII may contribute in part to the activation of the receptor (Groblewski et al., 1997; Rosenbaum et al., 2009). Furthermore, it has

TABLE 5

CCh potency (pEC_{50}) and curve-translocation (Log δ) values for the interaction between CCh and brucine at the $M_3K^{7.32}E$ mAChR after transfection with siRNA

Data are presented as the mean ± S.E.M. of four to five separate experiments performed in duplicate.

	Transfection Control	$G\alpha_q$ siRNA	$G\alpha_{12}$ siRNA
Ca^{2+} mobilization			
pEC_{50}	7.16 ± 0.20	7.44 ± 0.12	6.99 ± 0.16
Log δ	1.14 ± 0.23	0.41 ± 0.12*	1.01 ± 0.19
ERK1/2 phosphorylation			
pEC_{50}	6.33 ± 0.11	6.28 ± 0.12	6.64 ± 0.10
Log δ	0.82 ± 0.13	0.62 ± 0.14	0.16 ± 0.13*

pEC_{50}, negative logarithm of concentration agonist that generates 50% of the maximal agonist response; Log δ, logarithm of the ratio of the EC_{50} values of the allosteric modulator-treated and control CCh curves.

* $P < 0.05$ determined by one-way ANOVA with Newman-Keuls multiple comparisons post test between each transfection group in a single assay type.

been shown through disulfide cross-linking studies that amino acid residues in TMI interact with residues at the bottom of TMVII and that a large conformational change occurs at the bottom of TMVII upon application of agonist (Wess et al., 2008). There is also evidence that basic amino acid residues (such as lysine) in membrane proteins "snorkel" in the lipid and potentially interact with the charged head-groups in the phospholipid membrane (Mishra et al., 1994). Furthermore, a lysine residue at the juxtamembrane region of a TM helix has been shown to be important for coordinating the helix with the membrane and is also a determinant for the helical tilt (de Planque et al., 1999; Ozdirekcan et al., 2005). Therefore, perhaps, the $K^{7.32}E$ mutation in the M_3 mAChR alters the interaction of TMVII with the plasma membrane and, in turn, increases the propensity of the receptor to be activated/modulated by brucine. Irrespective of the mode of receptor activation induced by ligands acting at the $K^{7.32}E$ mutation, it is clear that the cooperativity between brucine and CCh is increased by the presence this mutation.

In conclusion, this study has provided evidence that the yeast signaling assay is a tractable and valuable platform for the determination of GPCR ligand-G protein functional selectivity profiles mediated by an allosteric ligand, as well as the provision of pharmacological parameters such as affinity, cooperativity, and relative efficacy estimates. We predict that this approach should be applicable to any GPCR than can be successfully expressed in yeast.

Acknowledgments

We are grateful to Dr. S. Dowell for provision of the yeast strains, Dr. J. Wess for provision of the rat $rM_3\Delta i3$ mAChR construct, and Dr. Michael Crouch for provision of the ERK1/2 assay kits.

References

Avlani VA, Gregory KJ, Morton CJ, Parker MW, Sexton PM, and Christopoulos A (2007) Critical role for the second extracellular loop in the binding of both orthosteric and allosteric G protein-coupled receptor ligands. *J Biol Chem* **282:**25677–25686.

Baker JG, Hall IP, and Hill SJ (2003) Agonist and inverse agonist actions of beta-blockers at the human beta 2-adrenoceptor provide evidence for agonist-directed signaling. *Mol Pharmacol* **64:**1357–1369.

Ballesteros JA and Weinstein H (1992) Analysis and refinement of criteria for predicting the structure and relative orientations of transmembranal helical domains. *Biophys J* **62:**107–109.

Birdsall NJ and Lazareno S (2005) Allosterism at muscarinic receptors: ligands and mechanisms. *Mini Rev Med Chem* **5:**523–543.

Brown AJ, Dyos SL, Whiteway MS, White JH, Watson MA, Marzioch M, Clare JJ, Cousens DJ, Paddon C, Plumpton C, et al. (2000) Functional coupling of mammalian receptors to the yeast mating pathway using novel yeast/mammalian G protein alpha-subunit chimeras. *Yeast* **16:**11–22.

Brown JH, Del Re DP, and Sussman MA (2006) The Rac and Rho hall of fame: a decade of hypertrophic signaling hits. *Circ Res* **98:**730–742.

Buller S, Zlotos DP, Mohr K, and Ellis J (2002) Allosteric site on muscarinic acetylcholine receptors: a single amino acid in transmembrane region 7 is critical to the subtype selectivities of caracurine V derivatives and alkane-bisammonium ligands. *Mol Pharmacol* **61:**160–168.

Caulfield MP (1993) Muscarinic receptors—characterization, coupling and function. *Pharmacol Ther* **58:**319–379.

Christopoulos A (1998) Assessing the distribution of parameters in models of ligand-receptor interaction: to log or not to log. *Trends Pharmacol Sci* **19:**351–357.

Christopoulos A (2000) Quantification of allosteric interactions at G protein coupled receptors using radioligand binding assays. *Curr Protoc Pharmacol* **11:**1.22.1–1.22.40.

Christopoulos A, Lanzafame A, and Mitchelson F (1998) Allosteric interactions at muscarinic cholinoceptors. *Clin Exp Pharmacol Physiol* **25:**185–194.

de Planque MR, Kruijtzer JA, Liskamp RM, Marsh D, Greathouse DV, Koeppe RE 2nd, de Kruijff B, and Killian JA (1999) Different membrane anchoring positions of tryptophan and lysine in synthetic transmembrane alpha-helical peptides. *J Biol Chem* **274:**20839–20846.

Dowell SJ and Brown AJ (2002) Yeast assays for G-protein-coupled receptors. *Recept Channels* **8:**343–352.

Erlenbach I, Kostenis E, Schmidt C, Hamdan FF, Pausch MH, and Wess J (2001) Functional expression of M(1), M(3) and M(5) muscarinic acetylcholine receptors in yeast. *J Neurochem* **77:**1327–1337.

Galandrin S, Oligny-Longpré G, Bonin H, Ogawa K, Galés C, and Bouvier M (2008) Conformational rearrangements and signaling cascades involved in ligand-biased mitogen-activated protein kinase signaling through the beta1-adrenergic receptor. *Mol Pharmacol* **74:**162–172.

Gnagey AL, Seidenberg M, and Ellis J (1999) Site-directed mutagenesis reveals two epitopes involved in the subtype selectivity of the allosteric interactions of gallamine at muscarinic acetylcholine receptors. *Mol Pharmacol* **56:**1245–1253.

Gregory KJ, Sexton PM, and Christopoulos A (2007) Allosteric modulation of muscarinic acetylcholine receptors. *Curr Neuropharmacol* **5:**157–167.

Groblewski T, Maigret B, Larguier R, Lombard C, Bonnafous JC, and Marie J (1997) Mutation of Asn111 in the third transmembrane domain of the AT1A angiotensin II receptor induces its constitutive activation. *J Biol Chem* **272:**1822–1826.

Iarriccio L (2008) *Allosteric Interactions at the M3 Muscarinic Acetylcholine Receptor*. Ph.D. Thesis. Polytechnic University of Catelonia. Barcelona, Spain.

Jakubík J, Bacáková L, Lisá V, el-Fakahany EE, and Tucek S (1996) Activation of muscarinic acetylcholine receptors via their allosteric binding sites. *Proc Natl Acad Sci USA* **93:**8705–8709.

Jakubík J, Krejcí A, and Dolezal V (2005) Asparagine, valine, and threonine in the third extracellular loop of muscarinic receptor have essential roles in the positive cooperativity of strychnine-like allosteric modulators. *J Pharmacol Exp Ther* **313:**688–696.

Kenakin T (1995) Agonist-receptor efficacy. II. Agonist trafficking of receptor signals. *Trends Pharmacol Sci* **16:**232–238.

King K, Dohlman HG, Thorner J, Caron MG, and Lefkowitz RJ (1990) Control of yeast mating signal transduction by a mammalian beta 2-adrenergic receptor and Gs alpha subunit. *Science* **250:**121–123.

Krejcí A and Tucek S (2001) Changes of cooperativity between *N*-methylscopolamine and allosteric modulators alcuronium and gallamine induced by mutations of external loops of muscarinic M(3) receptors. *Mol Pharmacol* **60:**761–767.

Lazareno S, Gharagozloo P, Kuonen D, Popham A, and Birdsall NJ (1998) Subtype-selective positive cooperative interactions between brucine analogues and acetylcholine at muscarinic receptors: radioligand binding studies. *Mol Pharmacol* **53:**573–589.

Leach K, Loiacono RE, Felder CC, McKinzie DL, Mogg A, Shaw DB, Sexton PM, and Christopoulos A (2010) Molecular mechanisms of action and in vivo validation of an M4 muscarinic acetylcholine receptor allosteric modulator with potential antipsychotic properties. *Neuropsychopharmacology* **35:**855–869.

Leach K, Sexton PM, and Christopoulos A (2007) Allosteric GPCR modulators: taking advantage of permissive receptor pharmacology. *Trends Pharmacol Sci* **28:**382–389.

Maillet EL, Pellegrini N, Valant C, Bucher B, Hibert M, Bourguignon JJ, and Galzi JL (2007) A novel, conformation-specific allosteric inhibitor of the tachykinin NK2 receptor (NK2R) with functionally selective properties. *FASEB J* **21:**2124–2134.

Mathiesen JM, Ulven T, Martini L, Gerlach LO, Heinemann A, and Kostenis E (2005) Identification of indole derivatives exclusively interfering with a G protein-independent signaling pathway of the prostaglandin D2 receptor CRTH2. *Mol Pharmacol* **68:**393–402.

May LT, Avlani VA, Langmead CJ, Herdon HJ, Wood MD, Sexton PM, and Christopoulos A (2007) Structure-function studies of allosteric agonism at M2 muscarinic acetylcholine receptors. *Mol Pharmacol* **72:**463–476.

Mishra VK, Palgunachari MN, Segrest JP, and Anantharamaiah GM (1994) Interactions of synthetic peptide analogs of the class A amphipathic helix with lipids. Evidence for the snorkel hypothesis. *J Biol Chem* **269:**7185–7191.

Nawaratne V, Leach K, Suratman N, Loiacono RE, Felder CC, Armbruster BN, Roth BL, Sexton PM, and Christopoulos A (2008) New insights into the function of M4 muscarinic acetylcholine receptors gained using a novel allosteric modulator and a DREADD (designer receptor exclusively activated by a designer drug). *Mol Pharmacol* **74:**1119–1131.

Olesnicky NS, Brown AJ, Dowell SJ, and Casselton LA (1999) A constitutively active G-protein-coupled receptor causes mating self-compatibility in the mushroom Coprinus. *EMBO J* **18:**2756–2763.

Ozdirekcan S, Rijkers DT, Liskamp RM, and Killian JA (2005) Influence of flanking residues on tilt and rotation angles of transmembrane peptides in lipid bilayers. A solid-state 2H NMR study. *Biochemistry* **44:**1004–1012.

Ridley AJ (2006) Rho GTPases and actin dynamics in membrane protrusions and vesicle trafficking. *Trends Cell Biol* **16:**522–529.

Rosenbaum DM, Rasmussen SG, and Kobilka BK (2009) The structure and function of G-protein-coupled receptors. *Nature* **459:**356–363.

Stewart GD, Sexton PM, and Christopoulos A (2010) Detection of novel functional selectivity at M3 muscarinic acetylcholine receptors using a *Saccharomyces cerevisiae* platform. *ACS Chem Biol* **5:**365–375.

Stewart GD, Valant C, Dowell SJ, Mijaljica D, Devenish RJ, Scammells PJ, Sexton PM, and Christopoulos A (2009) Determination of adenosine A1 receptor agonist and antagonist pharmacology using *Saccharomyces cerevisiae*: implications for ligand screening and functional selectivity. *J Pharmacol Exp Ther* **331:**277–286.

Urban JD, Clarke WP, von Zastrow M, Nichols DE, Kobilka B, Weinstein H, Javitch JA, Roth BL, Christopoulos A, Sexton PM, et al. (2007) Functional selectivity and classical concepts of quantitative pharmacology. *J Pharmacol Exp Ther* **320:**1–13.

Werry TD, Christopoulos A, and Sexton PM (2006) Mechanisms of ERK1/2 regulation by seven-transmembrane-domain receptors. *Curr Pharm Des* **12:**1683–1702.

Wess J, Eglen RM, and Gautam D (2007) Muscarinic acetylcholine receptors: mutant mice provide new insights for drug development. *Nat Rev Drug Discov* **6:**721–733.

Wess J, Han SJ, Kim SK, Jacobson KA, and Li JH (2008) Conformational changes involved in G-protein-coupled-receptor activation. *Trends Pharmacol Sci* **29:**616–625.

Yuan J, Rey O, and Rozengurt E (2006) Activation of protein kinase D3 by signaling through Rac and the alpha subunits of the heterotrimeric G proteins G12 and G13. *Cell Signal* **18:**1051–1062.

Address correspondence to: Prof. Arthur Christopoulos, Monash Institute of Pharmaceutical Sciences, Level 3, Building 4, 399 Royal Pde, Parkville, Victoria, Australia, 3052. E-mail: arthur.christopoulos@monash.edu